Radio Science

RESEARCH ARTICLE
10.1029/2022RS007591

Borealis: An Advanced Digital Hardware and Software Design for SuperDARN Radar Systems

K. A. McWilliams[1], M. Detwiller[1], K. Kotyk[1], K. Krieger[1], R. Rohel[1], D. D. Billett[1], D. Huyghebaert[1,2], and P. Ponomarenko[1]

[1]Department of Physics and Engineering Physics, University of Saskatchewan, Saskatoon, SK, Canada, [2]Department of Physics and Technology, The Arctic University of Norway, Tromsø, Norway

Key Points:

- The Borealis digital radar system is an advanced Super Dual Auroral Radar Network (SuperDARN) radar design using software defined radios
- The Borealis radar system can be retrofitted into existing conventional SuperDARN radar sites
- Borealis is capable of simultaneous multi-frequency operations and full field-of-view imaging

Correspondence to:

K. A. McWilliams,
kathryn.mcwilliams@usask.ca

Citation:

McWilliams, K. A., Detwiller, M., Kotyk, K., Krieger, K., Rohel, R., Billett, D. D., et al. (2023). Borealis: An advanced digital hardware and software design for SuperDARN radar systems. *Radio Science*, *58*, e2022RS007591. https://doi.org/10.1029/2022RS007591

Received 26 AUG 2022
Accepted 7 FEB 2023

Abstract The Borealis radar system is a hardware and software upgrade to the conventional Super Dual Auroral Radar Network radar system, which has been used since the early 1990s. The conventional system has hardware and software that is aging, and many components are no longer supported. Limitations of the conventional system limit radar and data techniques for scientific discovery. Using software defined radios, Borealis has improved the flexibility, capabilities, and security of the radar system. Borealis has improved system monitoring and diagnostics and enables more complex experiments. Borealis provides improvements in spatial and temporal resolution. The system can perform full field-of-view imaging, pulse phase encoding and simultaneous multi-frequency operations. With Borealis, data quality and system reliability has been improved. New radar and signal processing techniques are in development to further improve the capabilities of the system and of the data quality.

Plain Language Summary The Super Dual Auroral Radar Network (SuperDARN) has been in operation since the early 1990s. The Borealis system was designed as a hardware and software upgrade to the modified original radar system operated by SuperDARN Canada. Borealis has improved the flexibility, capabilities, and security of the radar system. With Borealis, data quality and reliability improvements have been achieved, and new radar and signal processing techniques are in development to further improve the capabilities of the system and the data quality.

1. Introduction

The Super Dual Auroral Radar Network (SuperDARN; Greenwald et al., 1995) is an international collaboration that operates ground-based high-frequency (HF) radars. The goal of the network is to measure the Doppler velocity of F-region ionospheric plasma by scattering HF radio waves from field-aligned plasma irregularities embedded in the drifting plasma. Comprehensive reviews of the scientific achievements of the SuperDARN and its collaborators have been written by Chisham et al. (2007), Lester (2014), and Nishitani et al. (2019). The collaboration began in the early 1990s with a handful of radars. It has expanded since then to nearly three dozen radars, as of the writing of this article. The expansion has significantly increased the global-scale spatial coverage of the network. The first radars observed auroral regions poleward of 60° geomagnetic latitude. SuperDARN now monitors ionospheric plasma drift from geomagnetic latitudes as low as 40° to the magnetic poles. By combining data from all available radars, a hemispheric snapshot of the high-latitude ionospheric convection pattern (e.g., Cowley & Lockwood, 1992) can be constructed every minute by fitting the available SuperDARN data using a spherical harmonic expansion method (Cousins & Shepherd, 2010; Fiori et al., 2010; Gjerloev et al., 2018; Ruohoniemi & Greenwald, 1996; Thomas & Shepherd, 2018). The convection patterns are assumed to be electrostatic solutions. The ionospheric electric potential distribution is directly related to the ionospheric convection pattern, because the velocity streamlines are parallel to the equipotential contours.

The majority of the SuperDARN radars have used, and many continue to use, designs, equipment and operating software from the initial days of operations (Greenwald et al., 1985). Limitations imposed on conventional operational parameters (integration time, sampling rate, spatial coverage, resolution, etc.) resulted from the trade-off between the SuperDARN's scientific objectives and contemporary engineering and computational capabilities at the time of the network's inception. The new radar system presented here makes it possible to relax or remove some limitations by applying modern advancements in digital radio design and data analysis techniques. Advances in computing power and radar electronics make it possible to modernize the software and hardware,

providing the potential to develop new radar techniques such as multiple-input-multiple-output measurements (MIMOs), simultaneous multi-frequency sounding, full field-of-view (FOV) beamforming for imaging, and finer detail pulse compression. Additionally, improvements in storage media and processing rates through the use of graphics processing units (GPUs) permit much greater sampling rates.

Newer digital transceivers, which are often called software-defined radios (SDRs), are able to digitize and process wide-bandwidth radio signals with fast analog-to-digital converters (ADCs) and field programmable gate arrays (FPGAs). The FPGAs are implemented within the transceiver, and they digitally process the signal in near real-time without the need for a phasing matrix of signal delay lines, which is part of SuperDARN's original system design. Commercial off-the-shelf devices exist for all of these purposes, with the capability of additionally incorporating GPS-disciplined clocks to improve the time accuracy of the measurements.

Advances have been made in the past two decades by SuperDARN partners in modernizing the conventional SuperDARN radars, focusing on the receiver and phasing matrix systems. The CUTLASS SuperDARN system made use of available transmitter duty cycle to broadcast on a second frequency and added a duplicate conventional receiver channel. This enabled near-simultaneous operation with two radar control programs at different frequencies (Lester et al., 2004). The availability of modern, supported hardware has led to some diversification of SuperDARN systems from the conventional system. Advances have been made using SDRs to digitize parts of the systems, making more complex radar operations possible (Bristow, 2019; Whittington et al., 2004; Yan et al., 2021).

SuperDARN's conventional implementation continues to produce high quality data to this day, but modernizing the system is becoming more critical for several reasons. One example is the digital receiver utilized by most SuperDARN radars, the Echotek GC214, which is no longer in production. Another example is the QNX4 operating system, which no longer has support or receives updates. These deprecated technologies make replacements and new developments difficult and perhaps impossible in the future. By replacing these technologies with widely available modern radio peripherals and supported operating systems, SuperDARN can more easily deploy new or replacement systems to its radars. The high degree of flexibility and the availability of software packages for these modern technologies allows researchers to more easily implement new radar techniques into their experiments. Borealis is a new open-source software and hardware design for SuperDARN radars (SuperDARN Canada, 2022). Its operating software has been written in a combination of modern C++, Python and CUDA programming languages, and the software runs on current (i.e., supported) Linux distributions.

The Universal Software Radio Peripheral (USRP) designed by Ettus Research is a comparatively inexpensive and accessible SDR. The first USRP-based SuperDARN radar design was developed by the SuperDARN group at the University of Alaska Fairbanks (UAF) and implemented at two SuperDARN sites (Bristow, 2019). The UAF system utilizes an Ettus Research X300 USRP device to record the in-phase and quadrature (IQ) signal voltages. The IQ data are processed into higher level SuperDARN data products, such as raw autocorrelation functions (RAWACF), and fitted (FITACF) parameters like Doppler velocity, signal-to-noise ratio, and spectral width. The new USRP system developed at the University of Saskatchewan, named *Borealis*, utilizes Ettus Research N200 USRP devices. The N200 USRP allows Borealis to perform all the necessary processing in real-time at the radar site, enabled in part due to the utilization of GPU processing. All USRP devices are supported by the USRP Hardware Driver (UHD), also developed by Ettus Research, meaning it would not be difficult to modify the software of the Borealis system to be compatible with the X300 device or other USRP devices. In addition to the UAF system, the TIGER radar system developed by the Department of Engineering at La Trobe University also utilizes one transceiver per antenna, but does not use USRP devices (Whittington et al., 2004).

This paper provides a description of the hardware, software, and data processing algorithms of the Borealis system. We will review the modified conventional SuperDARN control system that was in place at the five SuperDARN Canada radar sites (Clyde River, Inuvik, Prince George, Rankin Inlet, and Saskatoon), to compare and contrast with the Borealis system. The research group's headquarters at the University of Saskatchewan is very close to the radar at Saskatoon. For this reason, the Saskatoon site is used as the group's developmental site, where new hardware is tested and implemented, before being deployed at the more remote sites.

2. Conventional SuperDARN Systems

SuperDARN was designed to monitor the solar wind-driven ionospheric circulation pattern on a global scale using a large array of radars with overlapping FOVs synchronized to make full scans in unison (Greenwald

et al., 1995). A SuperDARN radar normally consists of 16 antennas in the main transmit/receive array and four antennas in the receive-only interferometer array. In the conventional system, one ADC digitizes the signals from two receiver channels (one for the main antenna array and one for the interferometer array) that have been combined and beamformed using fixed phase delays in the analog hardware before arriving at the receiver.

The convection monitoring scan mode, known as the Common Time Program, typically scans in 16 discrete beam positions through ≃50° in azimuth. Along a beam there are at least 70 measurement regions, known as range gates, that are typically 45 km in length. A complete scan through all beams takes place every 1 or 2 min, so that the radar sounds the same beam direction for ≃3.5 s or ≃7 s, respectively. This time is known as the beam dwell time or integration time. To accommodate requirements for both maximum measurable Doppler frequency shift and maximum range span, the radar transmits a sequence of irregularly spaced pulses whose backscatter echoes received by the main antenna arrays are combined into autocorrelation functions (ACFs) for each range gate (for more detail see, e.g., Greenwald et al. (1985) and Ponomarenko and Waters (2006)). A single pulse sequence is emitted and sampled during ≃0.1 s so that for 1- or 2-min scans echoes from N_a = 30–35 or 60–70 pulse sequences, respectively, are used to generate a single ACF. Similarly, signals received by the main and interferometer antenna arrays are combined into cross-correlation function (XCF) data. The ACFs and XFCs are recorded into 2-hr RAWACF files, which is a file format unique to SuperDARN.

The SuperDARN Canada radars are modified versions of the conventional system that was deployed at the Saskatoon radar site at the start of the SuperDARN collaboration. The transmit and receive operations of the radar control system were decoupled to two separate computer peripheral systems. The direct digital synthesis (DDS) system for transmit signal generation was controlled by a dedicated Linux computer. The Echotek GC214 receiver card sampled and filtered the received data and was controlled by a QNX4 computer. Both systems were interfaced with a SuperDARN software package known as the Radar Operating System (ROS), which ran on the QNX4 computer and which operated the radar by issuing directives to the DDS system and the receiver card. ROS also handled the data processing and writing the data to file.

The DDS system is a modification to the conventional SuperDARN system. The DDS system was first deployed in 2011 at the Inuvik SuperDARN radar and later installed at all Canadian SuperDARN radars. The DDS system was developed at the University of Saskatchewan in collaboration with the SuperDARN research group at Virginia Tech. The DDS system is a universal serial bus (USB) microcontroller-based signal generation system. It generates the beamformed transmit signals and the receiver mixing signals for receive-side beamforming. ROS communicates with the DDS computer over the network, sending information on radar pulse length, pulse sequence, frequency, phase offsets, and other information that the DDS requires to create the waveforms of the pulse sequence. The radar transmits a pulse sequence of irregularly spaced pulses of fixed lengths. Pulse waveforms are sent to the transmitters to be transmitted by each antenna, with the phase offsets on each waveform necessary for electronic beam steering.

The DDS system also sends beamformed mixing signals to the DDS phasing matrix—an analog system for beamforming and combining the received signals into arrays before they are digitized. The DDS phasing matrix consists of analog hardware (filters, mixers, amplifiers, switches for transmit blanking, a combiner, and coaxial cables that are carefully calibrated for electrical length to ensure phase matching between antenna channels) for each antenna array. The received antenna signals are mixed up to an intermediate frequency, and the appropriate phase offsets are applied to each signal. Switches attenuate the signal during transmit pulse times, and filters and amplifiers increase the signal level of the desired frequency band. Lastly, combiners combine the antenna signals into two beamformed signals, one signal for each of the main and interferometer antenna arrays.

To receive signals, the Echotek GC214 receiver card samples the beamformed signals from the main and interferometer arrays from the phasing matrix separately, using both of its two receive channels. The receiver uses a cascade-integrator comb design to filter the incoming signals. ROS can then save the incoming IQ voltages to file in the IQDAT format, as it is known, if specified, as well as process this data stream into the standard SuperDARN RAWACF format.

The DDS system was operational and performing well at all five SuperDARN Canada radars, but several issues in recent years prompted the desire to upgrade the system. First, parts of the system became outdated, creating an inevitable maintenance problem. The Echotek GC214 receiver card was no longer in production. The ROS software and the receiver card driver were both written to operate on the QNX4 operating system, which had

become deprecated. The continued use of QNX4 presented some network security risks and prevented modern timekeeping capabilities. The ROS software itself is also no longer being actively maintained, and documentation and knowledge resources surrounding this software are limited. Implementing new experiments using the ROS software can be time-consuming, as an advanced knowledge of ROS libraries is required to write radar control programs. Second, the use of a phasing matrix for analog beamforming creates a common and undetectable source of failure for individual antenna channels, since combining the antenna signals before digitizing masks hardware problems in the system (e.g., at an antenna) before the signals are combined. The phasing matrix is also an additional source of error, because the electrical paths from each antenna are affected by every analog hardware component. Non-linear phase offsets in the frequency band of interest are created that may present issues in determining the elevation angle of arrival of the signal, which is determined using the phase offset between the main and interferometer antenna arrays. Finally, the DDS system had limitations that were limiting the use of advanced radar techniques requested by users. The DDS system, for example, limits the pulse waveforms that can be used at one time to one of amplitude, phase or frequency modulation. It does not allow for, for example, phase encoding alongside the existing use of amplitude modulation that is used to form the pulses.

The length of the pulse sequence is limited in the modified conventional system by the microcontroller timers used to set delays between pulses. The number of pulses in a pulse sequence is limited to 20 pulses by the packet size limitation of the USB protocol. The receiver card sampling and filtering configuration is not very flexible and is obscured from the radar control program. Timing offsets, which are on the order of 1 s in the conventional system, and jitter from true GPS time limit the possibilities for synchronizing multi-instrument observations.

3. The Borealis Digital Radar

Borealis is a digital radar control system designed to replace the ROS configuration, including the DDS and phasing matrix, as well as the QNX4 computer and the Echotek GC214 receiver card. These multiple systems are replaced by a single integrated system, with both transmit and receive functions integrated into a common device. Borealis accomplishes this through the use of an array of modern SDR devices. The SDR devices are capable of producing arbitrary waveforms for transmit, of synchronized sampling of the antenna channels at high sampling rates, and of real-time digital signal processing (DSP) of the received samples. Synchronizing the 16 SDR devices is accomplished via common GPS-disciplined clock signals. A 10 MHz reference clock and a pulse-per-second (PPS) signal are distributed to all SDRs. The computing technology used is able to filter, decimate, beamform, and correlate the high-rate data into the SuperDARN RAWACF data format for multiple simultaneously received frequencies. Timekeeping is also improved through the use of a GPS-disciplined clock and a modern Linux operating system that can utilize the Network Time Protocol. The Borealis system does not replace the existing transmitter and antenna designs. Borealis is designed to interface with the existing SuperDARN transmitters. Borealis has been deployed at sites with the original SuperDARN log-periodic antennas (Greenwald et al., 1995) and at sites with the more modern twin-terminated folded dipole wire antennas (Custovic et al., 2011, 2013; Sterne et al., 2011).

The signal processing performed by Borealis is computationally demanding, and the use of modern computing hardware and software packages has made the high sampling rate possible. Care has been taken in the development of Borealis to improve software efficiency and flexibility for the system, and this is aided by access to the multitude of software packages available on modern Linux systems. The Borealis control software has been built with more complex radar experiments in mind. Additionally, modern storage technology allows the data to be stored with increased precision, so the widely used and well-supported HDF5 file format (The HDF Group, 1997–2020) was chosen.

In the following sections, we will detail the hardware and software design of Borealis to meet the needs of modern radar operations. Additional documentation is provided at https://borealis.readthedocs.io.

3.1. Physical Components

The Borealis digital radar control system has been designed with increased capabilities in mind, including multi-frequency transmit and receive, flexible pulse sequences, GPS timestamped transmission and reception, multi-static operation, imaging, and ease of use for the end user. To achieve these objectives, the hardware components were carefully selected. A comparison graphic of the Borealis equipment rack with the modified

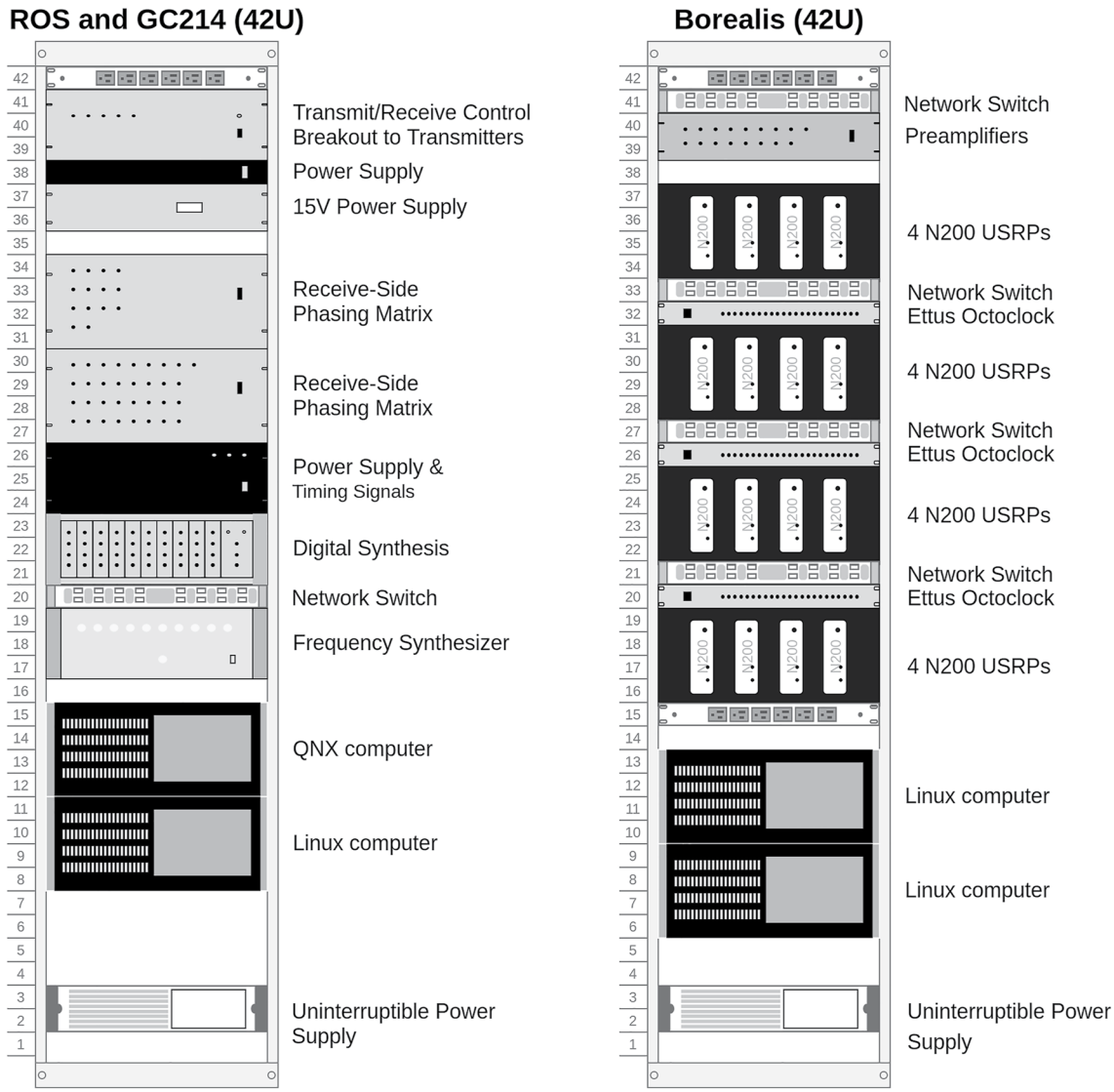

Figure 1. Schematic representation of the modified conventional Super Dual Auroral Radar Network direct digital synthesis equipment rack (left) and the Borealis equipment rack (right).

conventional system at the Saskatoon SuperDARN site is shown in Figure 1. The one rack of Borealis equipment has the same footprint as the equipment it replaces in the conventional system, making it possible to retrofit a Borealis system in an existing SuperDARN radar control building.

The Borealis digital radar control system comprises 16 N200 USRP devices mounted on four rack-mount shelves (see right-hand panel in Figure 1), along with the necessary peripherals, including three clocks for GPS-disciplined timing and synchronization, as well as network switches for data transfer to the Borealis computer, which is external to the rack. Each N200 device has one transmit channel and two receive channels when paired with the appropriate daughterboards, enabling transmit control of 16 antennas in the SuperDARN main array and as many as 32 receive antennas. Borealis uses 20 channels to digitize the 16 transmit/receive (T/R) signals from the 16-antenna main array and the four receive channels from the receive-only interferometer array. To achieve the desired data rates the Borealis computer, which is not mounted in the rack in Figure 1, was built using an Nvidia GPU with high parallelization, a high-core count CPU, a 10 GbE network interface, and adequate cooling and power to run continuously. The Borealis system replaced the modified conventional SuperDARN control system at the Saskatoon SuperDARN site in early 2019; at Prince George in September of 2019; at Clyde River in January of 2020; and at Rankin Inlet and Inuvik in September of 2021.

SuperDARN radars utilize phased antenna arrays, which means that all transmit waveforms provided to the transmitters require a well-defined phase angle with respect to each other. This can be achieved only if the SDRs providing the transmit waveforms are synchronized. Ettus Research documentation indicated that multiple N200 devices could be synchronized by using an Ettus Octoclock device, which provides a 10 MHz reference clock and PPS signal fan-out to up to eight devices. SuperDARN Canada radar sites operate with 16 transmitting and receiving antennas and four receive-only antennas, so a minimum of 16 N200 devices was required, as the N200s have only one transmit channel each. Therefore, more than one Octoclock device is necessary to synchronize all SDRs. To synchronize all N200 USRP devices and Octoclocks, a minimum of three Octoclock devices are required. The main Octoclock with a GPS disciplined oscillator supplies both a reference and a PPS signal to two secondary Octoclock devices, which then supply the reference and PPS signals to each of the 16 SDRs. With this setup, the electrical path length for the reference clock and PPS signals is the same for each SDR, as necessary for proper synchronization.

The N200 USRP devices contain a mainboard onto which daughterboards are inserted, based on the use case of the device. One daughterboard for transmitting signals and one daughterboard for receiving signals are used. For SuperDARN the Ettus Research LFTX (transmit) and LFRX (receive) daughterboards are sufficient, as they have a usable bandwidth from 0 to 30 MHz, covering the typical SuperDARN frequency band of 8–20 MHz. The LFTX and LFRX models of daughterboards do not contain any local oscillators, which would complicate phase synchronization between the N200 USRP devices. The N200 devices are factory shipped with only two bulkhead Sub-Miniature version A (SMA) outputs on the front panel, and one on the rear. Clean cable management, as well as a connection to the existing transmitters, dictated adding a SMA port on the front of the devices, as well as a DE-9F port on the rear to carry transmitter control and status signals between the N200 USRP devices and the transmitters. In addition, four extra timing/debug signals are routed to the rear of the case to bulkhead SMA connectors, and four indicator LEDs are routed to the front of the case. In total, there are an extra five bulkhead SMA connectors, one DE-9F connector and four 5 mm LED indicators added to the case. A custom printed circuit board (PCB) was added to the inside of the N200 cases to control front-panel indicator LEDs, to send and receive transmitter control and status signals, and to provide debugging signals.

To have a wide enough bandwidth for streaming samples to and from 16 N200 USRP devices with 10 Gbps connection to the computer running the Borealis software, a 5 MHz bandwidth was implemented. A 5 MHz sampling rate is used along with 16 bit in-phase (I) and 16 bit quadrature-phase (Q) samples. The data rate through this connection is 10 Mbps for each channel. With 20 channels, the single connection must be able to handle 200 Mbps. This equates to roughly 1.5 Gbps, before accounting for overhead. This data rate is facilitated via a 10 Gbps PCIe ethernet card. Specifically, the Intel X550 (1 or 2 port version) chipset was found to work well. The 10 Gbps PCIe card is connected to a 10 Gbps network switch. Both the eight-port NetGear XS708E-200NES and the eight-port NetGear XS708T network switches were found to work well. Three of the network switches daisy-chained together provide enough Ethernet ports to connect all 16 N200 devices. The 28-port NetGear XS728T network switch that had enough ports for all N200 devices but dropped too many packets when tested.

Processing a 5 MHz bandwidth of samples from 20 receive channels in real-time requires a specialized software and hardware setup. To accomplish the filtering and decimating of all these samples, an Nvidia GPU, along with the CUDA application programming interface, were used. In addition to a highly parallelized DSP software module, the planned-for flexibility of Borealis dictated modularized software. Many software modules are running at once, and to keep up with the demands of the software, a high core-count CPU is used. The Intel i9 series has been found to work well.

3.2. N200 Modifications

As mentioned above, several modifications were made to the N200 devices to integrate with the existing system, to provide real-time transmitter telemetry, and to provide visible indicators for the status of the N200s. These are LED indicators on the front panel, a rear transmitter interface connector, four rear SMA outputs, and a single front addition for the transmit SMA connector.

3.2.1. Visible Diagnostics

Four LEDs were added to each N200 USRP front panel. Each LED indicates a status of the USRP. The red TX-Only LED is active when the N200 is in transmit-only mode and not receiving. This indicates an error state.

The yellow IDLE LED is active when the N200 is neither transmitting nor receiving. This state occurs before the N200s have been configured by the driver, therefore indicating an intermediary state. The green RX LED is active any time the N200 is receiving. This should always be the case when running a regular experiment. The blue TX LED is active when the N200 is transmitting. During regular operation, transmission occurs every few milliseconds, so the LED should be flickering.

3.2.2. SMA Timing Signals

There are four single-ended timing signals generated by the modified N200 via female SMA bulkheads on the rear. These signals can be used for troubleshooting or for controlling transmitter T/R switches. They can be configured active-low or active-high by the Borealis software. The RX-Only signal is active when the N200 is receiving, but not transmitting. The IDLE signal is active when the N200 is neither receiving nor transmitting. The TX-Only signal is active when the N200 is transmitting, but not receiving. The T/R signal switches polarity when the N200 switches from transmitting and receiving to just receiving, or vice versa.

3.2.3. Transmitter Interface Connector

Most existing SuperDARN Canada sites have an available transmitter control cable, which provides a D-Subminiature DE-9M plug with all four transmitter interface differential signals routed to the connector. The mating socket (a panel-mount DE-9F) was incorporated into the N200 modifications to properly interface with the existing transmitter hardware.

3.2.4. Transmitter Telemetry and Control

In order to properly interface with the existing conventional transmitter hardware at each SuperDARN Canada site, a custom Transmitter Input-Output (TXIO) PCB is installed in each of the 16 N200 USRP devices. The TXIO PCB translates single-ended LVCMOS signals originating from the FPGA of the N200 devices to the differential signals required by the SuperDARN transmitters, as well as translating the diagnostic differential signals originating from the SuperDARN transmitters to the single-ended LVCMOS signals that the FPGA of the N200 devices require. There are two diagnostic signals generated by the transmitters: AGC (Automatic Gain Control) Status and Low Power. There are two control signals that the transmitters expect to receive: Test Mode and T/R.

AGC Status: The AGC status signal is a differential output from the AGC boards located within the transmitters. It indicates when there is a problem with the transmitter or when the transmitter is in test mode. The AGC status signal is measured in real-time by the Borealis software. If the AGC signal is active, it will turn off the radio frequency (RF) output on the AGC board, preventing any RF transmissions. In other words, if this signal is active, then the transmitter is not transmitting. It is generated by a logical AND ($\wedge$ operator) of the following four signals on the AGC board with a SN75183 quad differential line driver. The *500V_OK* signal indicates that the 500V line that back-biases two of the four HPTR switch PIN diodes during transmit is of a sufficiently high voltage. The *SWR_OK* signal indicates that the reverse power is not too high, that is, that the SWR of the antenna and feedline is low enough to not cause damage to the transmitter. It is active when the returned power is more than 50% of the full range, as visible on the transmitter's power monitor's red LED bar graph. The *TR_OK* signal indicates that there has been a T/R pulse within the last 150 ms. It is generated with a SN74LS123 monostable multivibrator, and an R/C combination of 22 kΩ/22 μF to generate the appropriate time constant. In general, this is a long enough time period to allow reasonable pulse sequences to be transmitted. It does impose an upper limit on the value of the multi-pulse increment value, or tau value. The *TEST* signal indicates if the transmitter is in test mode or not. It is a differential input to the AGC boards that is received by a differential line receiver, the SN75182.

Low Power: The low power signal is a differential output from the AGC boards. It indicates when the output power from the transmitter is below 80% of the full range as visible on the transmitter's power monitor's green LED bar graph and is measured in real-time by the Borealis software. It is generated by a SN75183 differential line driver on the Power Monitor board. If this signal is active, it is possible that the transmitter is still transmitting, albeit at a lower power level than nominal.

Test Mode: This signal is a differential input to the transmitter AGC boards. It is received by a SN75182 differential line receiver. While active, this signal will prevent the transmitter from transmitting, and thus the Low Power and AGC Status signals will become active if the associated circuitry is not damaged, therefore this signal can be utilized remotely by Borealis software to test a subset of the transmitter circuitry.

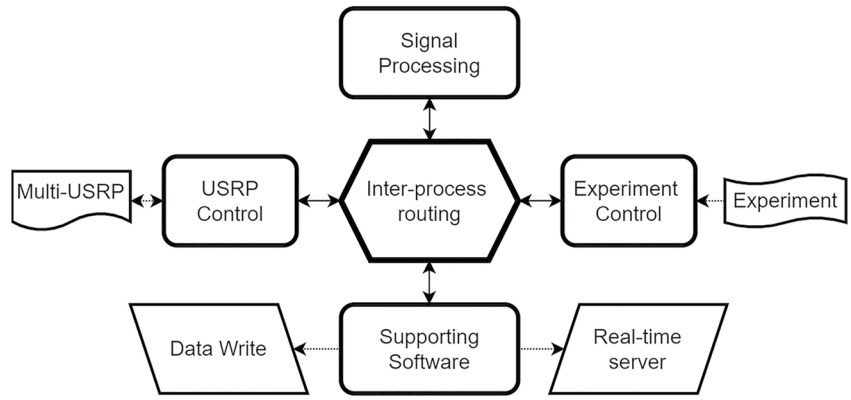

Figure 2. A block diagram depiction of the software structure for the Borealis system. There are four main categories of software modules: (i) experiment control, (ii) Universal Software Radio Peripheral control, (iii) signal processing, and (iv) supporting software. The different categories communicate through an inter-process routing system. Each software category contains multiple software modules, where a detailed description of each of the blocks in the diagram is provided in Sections 4.1–4.4.

Transmit/Receive (T/R): This signal is a differential input to the transmitters and is used by multiple transmitter modules. It is generated by using a feature of the N200 devices called "Automatic Transmit/Receive" and translated into a differential signal by the custom TXIO PCB. This signal switches the transmitter between transmit and receive modes, and is monitored by the AGC board to ensure that it is switching periodically.

4. Borealis Software

The Borealis software consists of software modules that work together in a pipeline to achieve a high level of parallelism. Parallelism is needed to ensure that the system can handle the high data rates from the USRPs while generating the internal logic needed to run experiments. The Borealis software modules can be grouped into four main categories: (a) experiment control, (b) USRP control, (c) signal processing, and (d) supporting software. The block diagram in Figure 2 is an overview of the main software categories and how they are interfaced. The communication between software modules is done using a routing process rather than components directly interfacing with each other. Details are expanded upon below.

The software was designed to best utilize the capabilities of the USRP system and to offer more flexibility in designing SuperDARN experiments. One of the core design philosophies was to create a system that places as few limitations on the users and the hardware as possible, to enable new and developing radar techniques in the years to come. The system is designed to abstract as much of the inner workings of the control system as possible. This choice allows users to write simple or complex experiments utilizing the radar techniques of their choice without needing detailed knowledge of how the system is implemented.

4.1. Experiment Control

The experiment control module (see Figure 2) contains multiple Python modules, including the experiment provided by the user, along with the software that controls how the system will operate to run the experiment. Experiments are written as Python classes, with attributes that define how the radar is to be run during an experiment. Among the attributes, the experiment includes a dictionary of one or more configurations that have been named experiment "slices." Borealis slices are objects that store different parameters such as frequency, pulse sequence, integration time, etc. A Borealis experiment contains one or more slices, and each slice produces its own data set. The slices can run concurrently, sequence by sequence, integration period by integration period, or scan by scan. In this way, the Borealis system can replicate the conventional SuperDARN operations, or it can run more complex modes, such as concurrent slices running the conventional SuperDARN scan on different frequencies.

At run-time, the control software will load the experiment and translate the user parameters into lower level objects and implementation details of the system. Borealis operations are structured to utilize the generalized

SuperDARN concepts of sequences of pulses; repetition of sequences during averaging periods, and averaging periods run sequentially in scans. The experiment control software reads the Python experiment class that is specified to run. Using the slice configurations and the interfacing information in the experiment class, the experiment control software builds the *Scan*, the *AveragingPeriod*, and the *Sequence* Python objects. Experiments consist of nested levels of scans, which are composed of averaging periods, which are composed of pulse sequences. The software iterates through the scans, averaging periods, and sequences.

As the control software cycles through the nested level of scans, averaging periods and sequences, it will use the data stored in those objects to generate the information needed for other aspects of the system, such as USRP configuration (center frequencies, transmit pulse samples, etc.), signal processing configuration (filter coefficients, beamforming phase angles, etc.) and metadata for data files.

Using one slice, Borealis can perform sequential scans of various beam positions, which matches the performance of the conventional ROS system. In each beam direction, the radar transmits and receives a series of pulse sequences within a specified time. This time is known by several names, including the integration time, the averaging period, or the beam dwell time. The pulse sequences from one beam direction are processed into ACFs and then averaged together. As an example, in the global convection scan mode the radar sweeps across the field of view in 1 min, transmitting and receiving in 16 sequential narrow beam directions. Along each beam direction, the radar transmits an irregularly spaced sequence of pulses, receives the backscattered power, processes the received data, and averages the pulse sequence data obtained in 3.5 s. The next full scan starts at the next 1-min boundary.

A key strength of the slice objects is that they are simple to configure. Configurable parameters include, for example, which antennas will transmit or receive, the number of ranges to sample, beam directions, or pulse sequences. These alone allow for different types of experiments to be designed. The flexibility increases with the different ways that slices can be interfaced. An example of a three-slice experiment is as follows. Two slices run concurrently, each slice running on its own frequency and transmitting on a subset of the available antennas. This is scan-interfaced with another slice that runs a standard 16-beam, 3.5 s averaging period, 7-pulse sequence scan. Running this experiment would generate three separate data files, one for each slice. This experiment makes it possible to compare new methods with traditional experiments in near-similar conditions.

4.2. USRP Control

The USRP control software is a C++ driver that controls the operation of the USRP N200 transceivers. The driver utilizes Ettus Research's UHD to configure the devices for SuperDARN operations. On startup, the driver software uses some radar site-specific options to initialize the N200s. All run-time control parameters are defined by the experiment control.

The driver is a multi-threaded program. There is a main thread, a transmit thread and a receive thread. Threads are used so that transmit and receive capabilities can be used simultaneously. The main thread is responsible for initializing the N200 devices with options, such as setting which physical N200 devices and channels to use, which General Purpose Input/Output pins to use for timing signals, and which GPS timing source to use for the N200s. The initial configuration is performed once at the start of run-time and then persists during operation. When the main thread finishes initialization, it spawns the transmit and receive threads.

4.2.1. Transmit Thread

The transmit thread is responsible for handling the transmit capabilities of the N200s. For every pulse sequence, the transmit thread obtains the sequence parameters and metadata from the experiment control, such as the center frequency, the pulse samples for each antenna, and the relative timing of when to send each pulse in the sequence. The parameter details are used to output the correct pulse waveforms with the correct timing.

The transmit thread first uses the sequence parameters to tune both the transmit and receive USRP center frequencies. In the current implementation, the transmit thread tunes both the transmit and receive frequencies so that the tuning operations are synchronized. The transmit thread tunes the receiver so that the receiver thread does not need to interrupt continuous sampling. Uninterrupted receive sampling leads to fewer errors and is described in more detail in the receive thread section.

When generating transmit waveforms, the N200 USRP devices expect a buffer of digital waveform samples and a future timestamp at which to trigger the output of the waveform. The N200 converts the buffer of complex

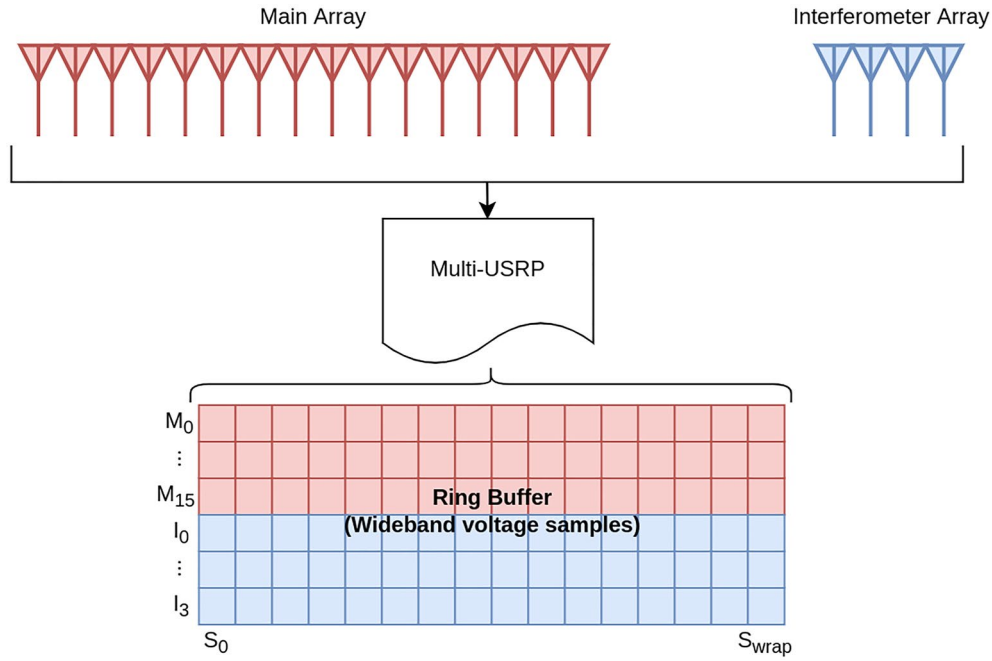

Figure 3. Received signal sampling and the ring buffer implementation. Signals received at the antennas travel through the receive path into the multiple N200 Universal Software Radio Peripheral devices, where they are sampled. The received samples are placed in the ring buffer (memory), with red cells containing data from the main array (shown here as cells from main antennas 0 through 15: $M_0 \ldots M_{15}$) and blue cells contain data from the interferometer array (shown here as cells from interferometer antennas 0 through 3: $I_0 \ldots I_3$).

samples to a RF signal via digital radio techniques. The buffers of transmit samples for each antenna are generated by the experiment control, but the experiment control only uses fundamental lag spacing and the pulse sequence to generate relative time spacing between each pulse. After the N200s have been tuned, the transmit thread uses the timestamp of the most recently received sample as the current time and uses the relative timing between pulses to calculate the true time to send each pulse. The pulse sequence as a whole has a 5 ms delay added to give the operating system time to send all the samples over the network to the N200s. The delay was determined empirically and may be modified.

The thread then waits for all samples to be transmitted before sending system information about the transmitted sequence to the signal processing software. The complete process of transmitting a sequence is repeated for each new sequence generated by the experiment control.

4.2.2. Receive Thread

The receive thread is used to sample the receive-path signal using the N200 USRP devices. While the N200s can perform the high sample rates required for continuous sampling of the wideband signal from the receive path, time-triggered receiving at the rates required by Borealis resulted in frequent errors and dropped samples. A continuous-receive ring buffer system was implemented to minimize dropped samples. The continuous sampling to the ring buffer requires a way to identify the valid samples in the ring buffer for data processing. The timestamp at which sampling began is used as a reference for indexing the ring buffer. The signal processing software uses this and the timestamp of the beginning of a transmit pulse sequence to extract valid samples for that sequence from the ring buffer for processing.

Figure 3 illustrates how each USRP receive channel maps to the ring buffer implemented in memory for that channel. In the multi-USRP system, there is an N200 receive channel for each antenna. Samples from each of those N200 receive channels, designated $M_{0\ldots15}$ (red) for the main array antennas and $I_{0\ldots3}$ (blue) for the interferometer array antennas, are placed into their own ring buffer. Each square represents a sample, and for illustrative purposes only a few samples are shown. S_0 denotes the first sample in time when the ring buffer is initialized. S_{wrap} is the last sample in time before the ring buffer wraps around. S_{wrap} is equivalent to the length of ring buffer. By

knowing the exact time when the ring buffer was initialized and the exact time when the first pulse in a sequence begins to transmit, one can calculate the position in the buffer of the received samples for that sequence.

The sample offset S_{offset} is given by:

$$S_{\text{offset}} = \frac{t}{F_s} \bmod S_{\text{wrap}} \tag{1}$$

where F_s is the sampling frequency and t is the amount of elapsed time since the buffer was initialized to the time the start of the first pulse in a sequence was transmitted. S_{offset} is calculated as the remainder from dividing the number of samples by the length of the ring buffer.

When the receive thread starts, it creates a shared memory section to use for the ring buffer. Received samples are put directly into shared memory that can be accessed by both the receive thread and the signal processing software. This minimizes the amount of inter-process memory copying. The receive thread continuously streams samples from each N200 channel into their respective buffers. Once streaming begins, the receive thread performs minimal actions besides streaming samples in order to minimize dropped samples. If the thread is delayed from continually receiving samples from the N200s, the N200 internal buffers will overflow and samples will be dropped. Because all received samples are timestamped, dropped samples do not affect the operation of the ring buffer, that is, all received samples are placed in the ring buffer in the correct memory location. If samples are dropped, the timestamps of the next successfully received samples will be used to skip ahead in the ring buffer. Although the operation of correctly indexing the ring buffer is self-correcting, the dropped samples can contaminate the pulse sequence data. The occurrence of dropped samples is very infrequent, and Borealis does not correct for contaminated sequences, but rather relies on the averaging of the ACFs to smooth out any ill effects of a contaminated sequence.

4.3. Signal Processing

The Borealis receive-side signal processing is performed in software once the complex raw voltage samples are recorded. The signal processing module is responsible for mixing to baseband, decimating, beamforming, and computing the ACFs. High-speed filtering and downsampling of the raw wideband samples from all antennas was one of the significant challenges of this system.

4.3.1. Filtering

The Borealis system is designed to receive a large bandwidth of the RF spectrum and then to decimate the signal down to one or more narrower bandwidths, depending on the control program. In order to filter and down-sample efficiently, a configurable cascaded filter design was implemented using a Python object to describe the filter design. Multiple sets of filter coefficients are generated for the multiple stages of filtering. The coefficients are stored as attributes in objects that describe the complete decimation scheme. The experiment configures the decimation scheme object or can leave it to default to a 45-km range scheme. Because multiple narrower bandwidths can be processed simultaneously, Borealis allows SuperDARN to operate using truly simultaneous modes for receiving at multiple frequencies.

In Borealis operations, each N200 receive channel receives at a 5 MHz sampling rate. While each individual N200 is capable of receiving at a rate of 10 MHz, at the time the system was implemented only 5 MHz proved to be reliable for the full system. Over the network, complex IQ samples are streamed as 16-bit integers, however the UHD is configured to scale the complex samples to 32-bit floating point numbers between 1 and −1 representing actual voltage values. A typical SuperDARN pulse sequence, such as the commonly used seven-pulse sequence, has a total sequence time of approximately 90 ms. At a total system sample rate of 100 Msps, Borealis will need to filter 9×10^6 samples (72 MB) in real-time—potentially multiple times if simultaneous frequencies are used—while samples for the next sequence are being collected. The most feasible way to process this kind of data in software and in real-time is to use efficient signal processing techniques that can be run on a GPU for high-speed processing.

The signal processing involved with decimating a wideband signal in real-time is extremely computationally demanding, and thus efficient DSP techniques and optimized software must be used. In the first stage of filtering, frequency translation is used to mix the desired frequencies to baseband. This can be done simultaneously

with the first stage of filtering by creating a bandpass filter and applying a phase correction after the fact. To accomplish this, a modified version of Frerking's filter technique for bandpass filtering (Frerking, 1994) was implemented. This filter technique is described in Section 4.3.2. After bandpass filtering is performed, one or more stages of low-pass filtering can be used.

4.3.2. Modified Frerking Method of Bandpass Filtering

The Borealis signal processing technique for decimation uses a modified application of Frerking's method (Frerking, 1994) to translate the samples to baseband, filter, and downsample. The method works by applying a phase shift to the filter coefficients prior to the convolution of those filter coefficients with the input samples to effectively accomplish a bandpass filter. A phase correction has to be applied after the convolution step, but this occurs after downsampling when fewer multiplications are required. This reduction in the number of computations enables the system to process the large data rates in real-time.

The method described by Frerking (1994) is applicable wherever the data are to be both mixed to baseband (i.e., frequency translation) and where data are filtered and decimated. This is traditionally accomplished in a multi-step process. The Frerking method creates a frequency-translating finite impulse response filter by applying the frequency translation to the filter coefficients rather than to the samples. The intention is to reduce the number of multiplication operations involved, as the number of filter coefficients is typically much smaller than the number of samples in the data. In addition to this, the filter convolution is only applied to those samples that are preserved after decimating.

In order to accomplish the same result as the conventional multi-step method of mixing the data to baseband, applying the filter, and lastly downsampling, the Frerking method applies phase shifts of linear increments to the filter, in effect creating multiple (let us say P) sets of filter coefficients that can be applied at increments of the decimation rate throughout the sample buffer. The number of phase shifts P that are necessary to apply is a lowest common denominator problem given by Frerking (1994):

$$PR\frac{f}{F_s} = \text{int}, \quad 1 \le P \le F_s, \tag{2}$$

where R is the integer decimation rate, f is the translation frequency, and F_s is the sampling rate.

Since Borealis is built to be configurable, we cannot ensure a favorably low common denominator, P, to ensure that the number of sets of coefficients necessary for Frerking's method would be reasonable in all future cases. In the worst case $P = F_s$, which is typically 5.0×10^6 for the Borealis system. Therefore, instead of applying the P phase shifts to the filter, the process was modified for Borealis by applying the incremental phase shift to the samples after the filtering and decimating is complete. This considerably reduces the number of operations, since the typical decimation rate for Borealis in the first stage of filtering is on the order of 10.

To compare the computational efficiency of the Frerking method and the modified method used in Borealis, we can formulate the number of multiplications involved in each method. Suppose N is the number of filter coefficients in the filter, and M is the number of samples in the output data after decimation. Frerking's method requires NP multiplications before convolution, to apply the phase shifts and create multiple filter sets. Alternatively, the modified method involves $N + M - \left\lfloor \frac{M}{P} \right\rfloor$ multiplications; N multiplications for mixing the filter prior to convolution, and $\left(M - \left\lfloor \frac{M}{P} \right\rfloor\right)$ multiplications after decimation to do a phase correction on those samples that require it.

For a small value of P and a large value of M output samples, the number of multiplications would be minimized by Frerking's method. However, the worst case for using Frerking's method is a large value of F_s, $M \ge F_s$, and an unknown f. Since Borealis is meant to be configurable, it assumes f is unknown. For an unknown integer value f and an unknown decimation rate (or where R is not a sub-multiple of F_s), processing would have to accommodate $P = F_s$, the largest possible value for the common denominator problem. Therefore, for $P = F_s$ the modified method is more computationally efficient when:

$$N + M - \left\lfloor \frac{M}{F_s} \right\rfloor < NF_s \tag{3}$$

where N is the number of filter coefficients, F_s is the sampling rate, and M is the number of output samples after decimation.

Frerking's method requires memory for storing P sets of N coefficients in order to be computationally efficient. The modified method is therefore more memory efficient in all cases where $P > 1$, because only one set of filter coefficients is ever required to be stored.

4.3.3. Borealis Filtering Implementation

The signal processing is performed by a C++ application that is responsible for decimating, beamforming and computing the ACFs. CUDA makes it possible to use a GPU as a coprocessor, allowing for high-speed filtering of the raw, high-bandwidth samples. Data products from various stages, including decimated samples for each antenna, beamformed decimated samples, and the ACFs, are sent to a Python process to be written to a file in real-time.

The signal processing software receives the metadata from the experiment control first. The metadata includes filter coefficients, sample rates for all decimation stages, and antenna phases for all beams. Pulse sequence metadata is also collected from the USRP driver software, such as the time-stamp at which receive-side sampling began, the timestamp at which the first pulse in the sequence was transmitted, and the number of samples for the sequence.

The GPU is configured using parameters generated by the experiment control. Borealis uses an NVIDIA 1080 Ti GPU (or better) with filtering implemented in CUDA. The GPU is configured to run in an asynchronous mode, so that more than one CUDA stream can be executed simultaneously. The GPU does not have enough computational resources to process data from more than one pulse sequence simultaneously. Copying the wideband samples from the ring buffer to the GPU can be done independently of computing, so significant time can be saved by asynchronously copying data from one pulse sequence to GPU memory while another one is being processed. The asynchronous mode also allows for a callback function that executes when the stream is finished without blocking the main thread from being able to initiate processing of new sequences. For readers not familiar with CUDA concepts or terminology, all details of CUDA programming can be found in NVIDIA's CUDA C++ Programming Guide (NVIDIA, 2016). The GPU operation of every new sequence can be summarized as follows:

1. Memory is allocated on the GPU device to hold the complex samples from the ring buffer, filter outputs for each decimation stage, and filter coefficients for each decimation stage.
2. Parallelized filtering convolution calculations are performed for each decimation stage.
3. A callback function is executed once the GPU is finished processing for post-filtering operations. Further details are described below.

To help visualize the implementation of filtering, Figure 4 is an illustration of the signal processing for a three-stage filter that produces output baseband samples at the desired rate for three experiment slices. This is one example of many possible implementations of filtering that can be used in Borealis. In the illustration, each small square represents a sample. The top block of samples represents the wideband samples in the ring buffer that are ready to be processed. For simplicity, only a subset of the ring buffer is shown. The samples from two main-array channels, labeled M_0 and M_1 (red), and the samples from two interferometer-array channels, labeled I_0 and I_1 (blue), are shown. This example represents an operational mode with three slices each centered on a different transmit frequency, which could be, say, 10, 11, and 12 MHz. Below the wideband samples in the illustration, the three groups of bandpass filter and downsample symbols represent the first stage bandpass CUDA kernel concurrently being applied to the wideband samples in the ring buffer. In this example, the first-stage filter produces three different output baseband data sets distinguished by the green, orange, and purple colors, corresponding to the three slices. Now that each slice data set is at baseband, the diagram shows two stages of CUDA lowpass kernels, represented with lowpass filter and downsample symbols. Each stage concurrently filters and downsamples each slice data set using one set of lowpass filter coefficients. The decimation rates shown in the downsample symbols in Figure 4 were arbitrarily chosen for the example. In reality, there are thousands of received samples that are processed simultaneously, and this diagram is a simplified depiction of the filtering and decimation processes.

Band-pass filtering is implemented using the modified Frerking method. Filter coefficients are mixed first with a translation frequency, the convolution is performed, and a phase correction is applied. A band-pass filtering CUDA kernel is used for the first stage of filtering in order to center on narrow bands around desired frequencies within the wideband that was sampled. In the bandpass filtering case, there is a single input data set and one output data set for each desired center frequency. The band-pass filtering CUDA kernel, represented in the first

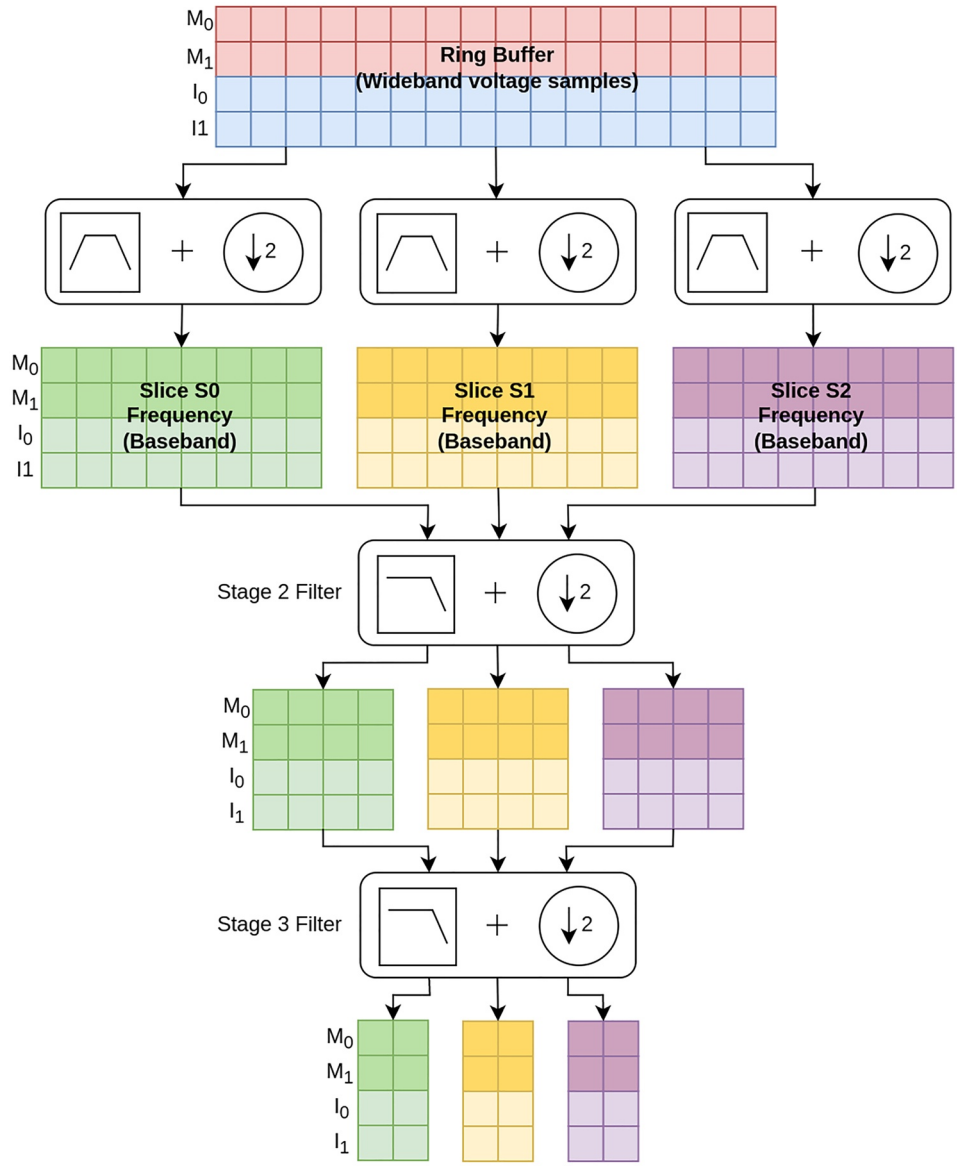

Figure 4. Diagram of a three-stage cascade filter implemented in the graphics processing unit. This example illustrates filtering three simultaneous experiment slices from the wideband voltage samples. This diagram includes input from only two main (red) and two interferometer antennas.

stage of filtering and decimation in Figure 4, is configured with a two-dimensional grid of CUDA blocks with the grid dimensions being the number of decimated output samples by the number of antennas. By structuring the CUDA blocks this way, we can perform convolution only on samples needed for the output and skip samples that would otherwise be dropped while down-sampling. Each convolution calculation for the output samples are independent of each other, meaning that each running kernel will, in parallel, calculate an output sample for one of the sampled antennas.

4.3.4. Beamforming and Autocorrelation Functions

In the conventional SuperDARN system, beamforming is performed in hardware using an analog phasing matrix. The Borealis system performs receive-side beamforming in software on the filtered and downsampled complex voltage samples from each antenna. The Borealis beamforming is performed on the received samples from one transmitted and received pulse sequence at a time. The received samples A from every antenna are superposed through a matrix operation to combine the received signals from the antennas and the phase angles of the antenna

array, where there is one phase value for each antenna. This constructive interference effectively "steers" the receive-sensitivity of the array in a particular beam direction. In Borealis the beamforming is implemented as a matrix multiplication, as follows:

$$\underset{n\times s}{\mathrm{B}} = \underset{n\times a}{\psi} \times \underset{a\times s}{\mathrm{A}} \tag{4}$$

where B are the beamformed samples, n is the number of beams, s is the number of samples, and a is the number of antennas (phase angle) values. For conventional SuperDARN operations, where one narrow beam sweeps through sequential beam directions, there are approximately $s = 300$ samples per pulse sequence, $n = 1$ for an individual beam direction, and $a = 16$ antennas in the main array and $a = 4$ antennas in the interferometer array. Beamforming is performed separately for the main and interferometer array data. Because the beamforming is implemented as a matrix operation, multiple simultaneous beams that is, $n > 1$, can be resolved very efficiently.

The beamformed signal produced by Borealis is of the same format as the beamformed signal produced by the conventional SuperDARN systems. The ACF of the Borealis beamformed signal can be calculated in the same manner as the ROS implementation of the conventional SuperDARN systems. Borealis optimizes the ACF processing by using matrix operations. While ACFs only need to be computed for specific combinations of voltage samples corresponding to radar pulses at desired ranges, correlations of all voltage sample combinations are computed using a highly optimized matrix operation. ACF lags that correspond to lags between pulses at each range are then selected from the resulting matrix, and the other lags are discarded. The same process applies to the cross-correlation of the signals from the main and interferometer antenna arrays.

4.4. Supporting Software

There are several software modules that play a smaller role in the system. Borealis consists of programs written in different languages, so inter-process communication is done using inter-process networking. To facilitate a pipeline system that performs smoothly, there is an application that acts as a router through which all communication flows. The primary purpose of the router application is to direct incoming packets from one process to their intended destination. Because all traffic flows through this process, it can also serve other purposes. The router application will throttle the throughput of the system to make sure that no application begins processing a new sequence before the rest of the system is ready. The router application also handles and logs error messages. Other supporting software includes an application for creating processed data files and an application for serving data to web applications in real-time.

5. New Operational Capabilities

The hardware and software of the Borealis system enable novel experiments and operating modes. In Borealis a 5 MHz wideband RF signal is digitized from each antenna and sent to a networked computer where the complex voltage samples are stored in RAM (the ring buffer). Once the complex voltage samples are in the ring buffer, many analysis techniques can be performed on the data. New capabilities made possible by Borealis include simultaneous multi-frequency operations, phase encoding and compression of the radar pulses, bistatic operations, adaptive beamforming and wide-field imaging.

The data processing example of multi-frequency operations was described in Section 4.3.3. The Borealis system uses a GPU to decimate and mix the samples down to baseband at one or more slice center frequencies with much smaller bandwidths. The current Borealis implementation of the RF signal processing makes it possible to operate simultaneously on different RF frequencies within the 5 MHz band. There are limitations in the current Borealis implementation to keep in mind when writing the control program. As an example, the bandwidth corresponding to each slice center frequency within the 5 MHz band must be the same due to the way the GPU processing is implemented, though this could be modified with the addition of another GPU. Another example is that the fastest sampling rate required for an experiment is what determines the sampling rate for all slices, resulting in possible oversampling depending on the operating modes being used. For example, 15 km range gate modes for SuperDARN require a faster sampling rate than the 45 km range gate modes. During the experiment setup of simultaneous 15 and 45 km range gate modes at different slice center frequencies, the Borealis system will be configured to sample at the faster rate for both slices. This results in the 45 km range gate mode being oversampled, even though

the experiments are at different slice center frequencies. Oversampling the incoming RF signal is preferable to undersampling the signal, to avoid information loss. Software has not yet been developed to account for oversampling operations when converting the complex voltage data to the RAWACF data format, and it is currently recommended that all simultaneous multi-frequency experiment setups use the same sampling rate.

The ability to record the raw voltage samples from each antenna separately is a capability that is not available in the conventional SuperDARN systems. Antenna-specific data are beneficial to troubleshooting system problems, as well as to testing the implementation of signal processing techniques. It allows different analysis methods to be applied to the same voltage data, providing the opportunity to test, verify and compare signal analysis implementations. Some diagnostic capabilities made possible by the implementation of Borealis include: rapid spectral power monitoring across the 5 MHz RF bandwidth, single-antenna RF path diagnostics, system phase calibration using RF noise generators, and individual RF path software-based phase and amplitude corrections. These diagnostic capabilities are not explored in detail here, but rather are just a few examples of how Borealis can improve SuperDARN operations.

Figure 5 illustrates the flow of data and where the new operational capabilities would be implemented in the receiver data flow. The blocks and the implementation of different experiments are described in detail below. It should be noted that, as illustrated in Figure 5, the system setup lends itself to parallelization. Most of the processing can be performed in parallel, resulting in minimal increases to the computation speed for each stage of expanded signal processing resulting from the more advanced radar experiments. This is important since the amount of data to process increases for each additional experiment capability that is implemented. The amount of data depends on the number of slices ($S\#$), ranges ($N_{S\#}$), and beams ($B_{S\#}$) implemented simultaneously for an experiment. In practice, data storage and network bandwidth to the radar sites become the limiting factors.

5.1. Simultaneous Multiple Frequency Operations

One of the capabilities of the Borealis system is truly simultaneous multiple-frequency operations. Simultaneous multi-frequency operations are not possible with the modified conventional SuperDARN system, though it has been implemented at the McMurdo SuperDARN radar with updated hardware and software (Spaleta et al., 2015). The Borealis system allows the transmission and recording of equal RF-bandwidth signals on multiple slice center frequencies within the larger 5 MHz sampled RF band. The processing of the 5 MHz signal received from each of the 20 antennas and the subsequent separation of the different center frequencies occurs in the GPU, as represented in Figure 5. RAWACF data are generated from the complex voltage data sets for each slice center frequency.

The most important observational result of multi-frequency measurements is the increase in the spatial coverage along the beam direction. At higher frequencies, the position of ionospheric echoes is located further away from the radar. Based on interleaved (sequential) two-frequency operations, two-frequency operations provides a 50%–75% increase in the range coverage. Another application of multi-frequency operations is oblique ground scatter ionograms, which provide essentially the same information as ionosondes.

Multiple frequency operation enables the simultaneous measurement of scatter from plasma density irregularities with different characteristic wavelengths. This can provide insight into the growth rate and phase velocity of plasma density irregularities in a similar volume (Kelley, 2009). Of particular interest to SuperDARN science, Borealis enables the comparison of simultaneous observations of the spectral width of the measured signal at different frequencies, similar to the non-simultaneous comparisons presented by Ponomarenko et al. (2007). The spectral width can be related to the decay time of plasma density irregularities (Ponomarenko et al., 2007). Analyzing data obtained using different transmitted frequencies can reveal information on the growth rate and diffusion rate of the plasma density irregularities at different characteristic wavelengths.

5.2. Full Field of View Beamforming and Imaging

The conventional SuperDARN system sweeps sequentially through 16 positions, with radiated power and receiver sensitivity concentrated in a narrow beam. A full scan is completed in 1 or 2 min. In contrast, Borealis can illuminate and sample the full SuperDARN FOV simultaneously, which we will refer to here as "imaging." Changes to both transmit and receive operations of the radar are needed for imaging. In conventional SuperDARN

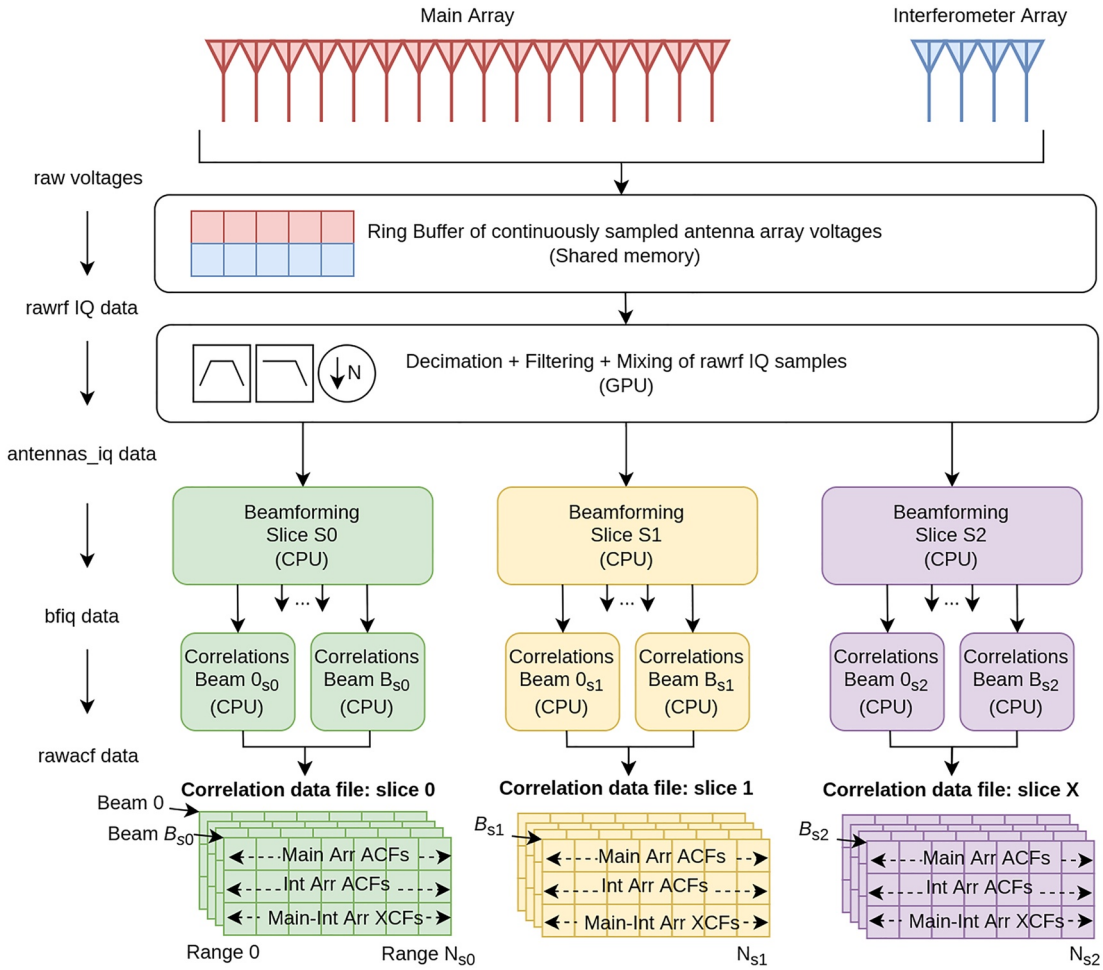

Figure 5. Diagram of an example implementation of modern capabilities for the Super Dual Auroral Radar Network Borealis system. The top three rows summarize the data flow for the received signal sampling from the antennas and the filter implementation, which were discussed in relation to Figures 3 and 4. After samples are received and placed into the ring buffer, the graphics processing unit decimates and mixes the 5 MHz sampled incoming signal for the separate slice center frequencies with much smaller sampling rates for each antenna. Each of the beam directions for each slice center frequency is then processed by the CPU to ultimately generate correlation data files, one for each slice *S#*. Further processing to deal with experiments containing pulse phase encoding techniques is described in Section 5.4.

radars, analog receiver systems beamform and combine the signals from all antennas before they are digitized. Borealis digitizes the complex voltage samples from each antenna before beamforming. The digitized samples from the GPU can be simultaneously beamformed into multiple beam directions using sets of phase angles for each antenna. This creates a beamformed data set that reproduces the conventional SuperDARN FOV, but the full FOV image can be determined in the time it takes to sample a single narrow beam for a conventional SuperDARN radar. The beamforming process occurs at the "Beamforming Slice $S_{\#}$" blocks in Figure 5. Imaging improves the temporal resolution along a beam direction and reduces spatio-temporal ambiguity across the FOV by creating a simultaneous full FOV image in one conventional beam dwell time. For conventional SuperDARN radars scanning through the full FOV, the temporal resolution along one beam direction is limited to the duration of a full scan.

The implementation of imaging will require modification of the conventional transmitter capabilities. The full FOV can be imaged by Borealis on the receiver side from the complex voltage data recorded from each antenna, but if a narrow beam like that from a conventional SuperDARN radar is being transmitted, the azimuthal extent of the image will be limited to the narrow width where transmitted power is being radiated. Using a wide-beam transmission with nearly uniform transmitted power across the FOV would be needed to obtain an image with similar sensitivity in all nominal beam directions. A potential drawback to full-field imaging with a broad beam from the conventional SuperDARN transmitters is that the effective radiated power (ERP) of the system is

decreased due to the transmitted power being dispersed over a larger area. While the transmitters have yet to be modified, a proof-of-concept test of full-FOV imaging was performed and will be discussed in Section 6.

The availability of complex voltage samples from each antenna provides an opportunity to improve the spatial resolution of the images by utilizing the Capon method (Capon, 1969), the maximum entropy method (e.g., Hysell, 1996), and compressed sensing (e.g., Harding & Milla, 2013), provided that some additional assumptions about the nature of the backscatter echoes are applied. Recently Bristow (2019) applied a similar technique to SuperDARN complex voltage samples obtained during a conventional (beam-scanning) operating mode. Recording the complex voltage data from each antenna individually also allows Borealis to do adaptive beamforming to produce a null in the direction of an interference/noise source and a maximum in the direction of the desired signal.

5.3. Multistatic Operations

Conventional SuperDARN radars are restricted to monostatic operations. With the goal of measuring overlapping components of ionospheric flow velocity, pairs of SuperDARN radars were built with overlapping FOVs when the geography of the radar locations made it possible. Given the large number of paired SuperDARN radar FOVs, the addition of a bistatic capability is highly desirable for expanding the network's observational potential. The main advantage of bistatic operations is that it provides an additional independent data set of velocity components measured along the direction of the bisectors of the crossed viewing directions from two radars (e.g., Rytov et al., 1988). The bistatic capability increases the effective number of radar units from two to four (by adding two bistatic setups to the two monostatic ones). This potentially improves the spatial coverage by filling the gaps in the monostatic data and, therefore, increases the likelihood of spatially coincident simultaneous observations. A bistatic setup requires each radar to operate at a different frequency to avoid cross-interference. This issue is readily resolved through Borealis' capability to process slices simultaneously at multiple center frequencies within the 5-MHz bandwidth. Another key factor is the ability to synchronize the timing between two sites. Borealis uses GPS timing units to synchronize each USRP N200 transceiver clock using PPS and 10 MHz clock signals. This restricts the timing error between different radar sites to within $\simeq$50 ns. This is adequate for implementing bistatic operations, as the shortest operational pulse duration is currently 100 μs.

A proof-of-concept test of a basic bistatic setup for SuperDARN radars was performed by Shepherd et al. (2020). This experiment included a single transmit-receive site and a receive-only site. The transmit-receive radar operated in a normal monostatic SuperDARN mode, while a second radar located some distance away operated in a receive-only mode. While the Borealis system is ready for operating in a bistatic mode, its implementation is not straightforward, as it requires expansion of the current spatio-temporal mapping of the multi-pulse patterns onto the bistatic case (when the transmitted and scattered signals do travel along one beam direction). Shepherd et al. (2020) bypassed this issue by synchronizing the beam orientations in such a way that the transmitting and receiving beams always intersected at a location equidistant to both radars. Such an operating mode provides bistatic data only at a single range for any given beam dwell time. In that respect, Borealis is capable of resolving this issue by illuminating the full field of view using a broad transmit beam, as described in Subsection 5.2.

Another complication with processing and interpreting bistatic data is that, in addition to the ionospheric and ground propagation modes, direct propagation between the two sites becomes possible. While the direct signal would be emitted and received by the side lobes at both sites, it may act as strong interference if the transmitter frequency lies below the maximum usable frequency for this propagation path. The presence of the direct propagation mode has been confirmed by Shepherd et al. (2020).

5.4. Pulse Phase Encoding and Compression

The SDR hardware and software of the Borealis system make it possible for a user to control the phase of transmitted pulses. This capability can be used to mitigate self-clutter in quasi-deterministic echoes (e.g., ground scatter) by randomizing inter-pulse and inter-sequence phasing in a manner similar to the technique proposed by Lehtinen et al. (1997). A thorough pilot study is needed, however, as this approach has not been tested on radars operating in the HF band.

Phase encoding enables pulse compression (Richards et al., 2010). Pulse compression is traditionally used at incoherent scatter facilities (Gray & Farley, 1973) to improve group range resolution without decreasing ERP, which

Table 1
Comparative Summary of Borealis Capabilities

Capability	Conventional SuperDARN	Borealis
Output data	Beamforming performed by analog filtering and mixing. ACF/XCF data for 16 beams recorded at site, with no capacity for post-processing	Received raw voltage data is recorded at each antenna, added capacity to post-process ACF/XCF data with different beam shape, scan configuration, integration time, etc.
Antenna pattern	16 narrow, fixed-width transmit-receive look directions (beams)	Flexible look directions and beam width configurations. Independent beamforming for transmission and reception
FOV sampling	Full FOV measured via sampling of 16 sequential narrow beam directions, resulting in a 1-min sampling rate along one beam direction	All beam directions can be sampled simultaneously, resulting in a 3.5-s sampling rate along one beam direction
Multi-frequency operations	Consecutive sounding at different radar frequencies. Narrowband RF signal at receiver allows one frequency to be received at a time	Simultaneous sounding at multiple frequencies enabled by the 5 MHz wideband RF received signal
Diagnostics	LED bulbs indicating good/bad status of transmitter systems visible to on-site personnel. On-site personnel to engage transmitter test-mode. Limited receive-path diagnostics at array level (2 receive paths—main and interferometer arrays)	Telemetry for transmitter health (low power, GPS status, system time, GPS time, etc.). Remote control of transmitter test-mode. Receive-path diagnostics at individual antenna level (20 receive paths)
Maintenance	Deprecated receiver card, out-of-date operating system with no support or security	Modern and available off-the-shelf parts, modern operating system with support and security
Software	C and shell scripts	C++, Python, CUDA, and shell scripts. Developed using Git and GitHub

is a problem faced by conventional SuperDARN systems when trying to improve range resolution. The pulse compression technique requires a broader signal bandwidth, so a detailed feasibility study would be required prior to its implementation to ensure compliance with a Borealis radar's radio spectrum license. Further investigation would also be required to determine the effects of ionospheric refraction on the efficacy of pulse compression for backscatter signals in the HF range.

5.5. Summary of New Operational Capabilities

The capabilities of the Borealis system, which are described in detail above, are summarized and compared with the conventional SuperDARN system in Table 1. We focus on the capacity for developing operational advancements, knowing that all future experimental configurations using Borealis cannot be anticipated at present. Given the open-source and user-friendly nature of the Borealis design, we anticipate investigations by many future users with as yet unknown experimental requirements.

6. Demonstration of Advanced Capabilities

We provide an example of Borealis' extended capabilities (see Table 1). The data were obtained during a test experiment performed on 7 February 2022 at the Clyde River SuperDARN radar. Between 16:00 and 20:00 UT the radar was operating in a full-FOV imaging mode. A wide transmission beam illuminated the full FOV. The wide beam was achieved by transmitting from only two adjacent antennas at the center of the main array. Based on simple simulations at a radar frequency 10.7 MHz, transmitting on two antennas was expected to illuminate the FOV with fairly good signal power within approximately $\pm 25°$ from the boresight direction. Only a relatively small 3–4 dB decrease in the antenna gain was expected near the edges of the conventional 16-beam FOV.

While only two transmitters were used during this test experiment, all receivers in the main and interferometer array were receiving. The received samples from all antennas were post-processed to form RAWACF data along the 16 conventional beam directions using the integration time of $\simeq$3.5 s. For a conventional SuperDARN system, scanning sequentially through 16 beam directions and integrating for 3.5 s per beam results in the 1-min full-FOV scan duration. The full-FOV imaging test experiment resulted in RAWACF data along 16 simultaneous beam directions during a scan time of 3.5 s.

The reduction of backscattered power due to transmitting from only 2 of 16 antennas over a broad field of view is expected to be about 18–20 dB. As SuperDARN radars regularly observe echoes with signal-to-noise ratio (SNR)

in excess of 35–40 dB, we expected a significant amount of backscatter with SNR in the 15–20 dB range. Our estimates have been confirmed by observations, as illustrated by the imaged "fan" plot of SNR during a 3.5 s integration time in the top left panel of Figure 6. The measurements from all beam directions were obtained simultaneously. The peak SNR values are above 30 dB, and there is no noticeable SNR "roll-off" at the edges of the FOV. As all beam directions were illuminated simultaneously, the test experiment provided an immediate 16-fold improvement in temporal resolution, that is, a full FOV sampled in 3.5 s versus the conventional 1 min scan. The top right panel in Figure 6 is a fan plot of the line-of-sight velocity components, with blue/cyan colors denoting plasma flow toward the radar (positive values) and red/yellow away from the radar (negative values). The image is typical for a near-noon ionospheric pattern, with the region of echoes near the radar consistent with antisunward flow across the FOV (toward the top of the plot). The region of echoes closer to the radar (blue-cyan-green, up to −1,000 m/s) are typical of 1/2-hop high-velocity echoes from ionospheric irregularities at closer ranges. The light green (low velocity) region of scatter at farther range gates is consistent with 1-hop scatter from the Earth's surface.

The advantage of having higher temporal resolution along all beam directions is illustrated by the bottom three rows in Figure 6, showing time-range plots of SNR (top row), line-of-sight velocity (middle row) and elevation angle (bottom row) observed by the south-most beam 0 direction measured from 19:00 to 19:20 UT. The data in the left panels have the 3.5-s sampling rate that is achieved through imaging. The data in the right panels are intentionally downgraded, such that only every 16th sample of the imaging data is included to emulate the 1-min time-resolution along a beam of a conventional SuperDARN scan. The imaging data on the left reveal much finer temporal structures like the diagonal stripes between range gates 10 and 20, which are indiscernible in the conventional data.

7. Summary and Conclusions

The Borealis digital radar system is an advanced SuperDARN radar design that replaces aging and deprecated SuperDARN operating systems and hardware components. Borealis produces data files that are compatible with conventional SuperDARN systems and software. Borealis can be retrofitted into existing conventional SuperDARN radar hardware setups. As of September 2021, the Borealis system has been installed and is running at all five SuperDARN sites operated by the SuperDARN Canada group at the University of Saskatchewan. Borealis data from all five Canadian SuperDARN radars are being shared with SuperDARN partners through the collaboration's international data distribution system.

Borealis is designed to handle the high data rates involved in digitizing and processing a 5 MHz wideband RF signal from each antenna. The system uses a GPU, a ring buffer, and the implementation of a modified Frerking method (Frerking, 1994) to optimize and have a highly reliable data processing workflow. Borealis has already proven itself useful for its ability to monitor and diagnose technical problems remotely. This includes visibility into the performance of individual antennas, which is not possible in conventional SuperDARN systems. Non-deprecated software and hardware improves cybersecurity and maintenance, due to the availability of regular updates and replacement parts. Improving the reliability of the system improves the reliability of the data. Key issues can be pinpointed and corrected in a timely manner, which simplifies identification of related environmental factors such as power outages, lightning strikes, equipment failures, etc.

The scientific objectives of the Borealis project were to improve ionospheric diagnostics. Multi-frequency capabilities allow users to expand radar coverage, to access multiple ionospheric irregularity scale sizes simultaneously, and to operate as oblique ionosondes or in multistatic configurations. The user-friendly nature of the Borealis system has allowed us to quickly implement proof-of-concept experiments to test some of these techniques. Due to the modular nature of the system, testing can be performed on each implementation of new operational capabilities without requiring changes to the other filtering and analysis software. This enables relatively straightforward identification and correction of issues, with the changes constrained to a block of software and/or hardware. The ability to capture the complex voltage samples from each antenna enables users to post-process (downsample, beamform, and analyze) data in more than one way after the data are collected. This essentially allows users to "run" more than one experiment configuration with the same data set.

Because the system is modularized, new capabilities can be implemented individually or in combination. For example, a user could combine capabilities and operate with full FOV imaging using more than one frequency

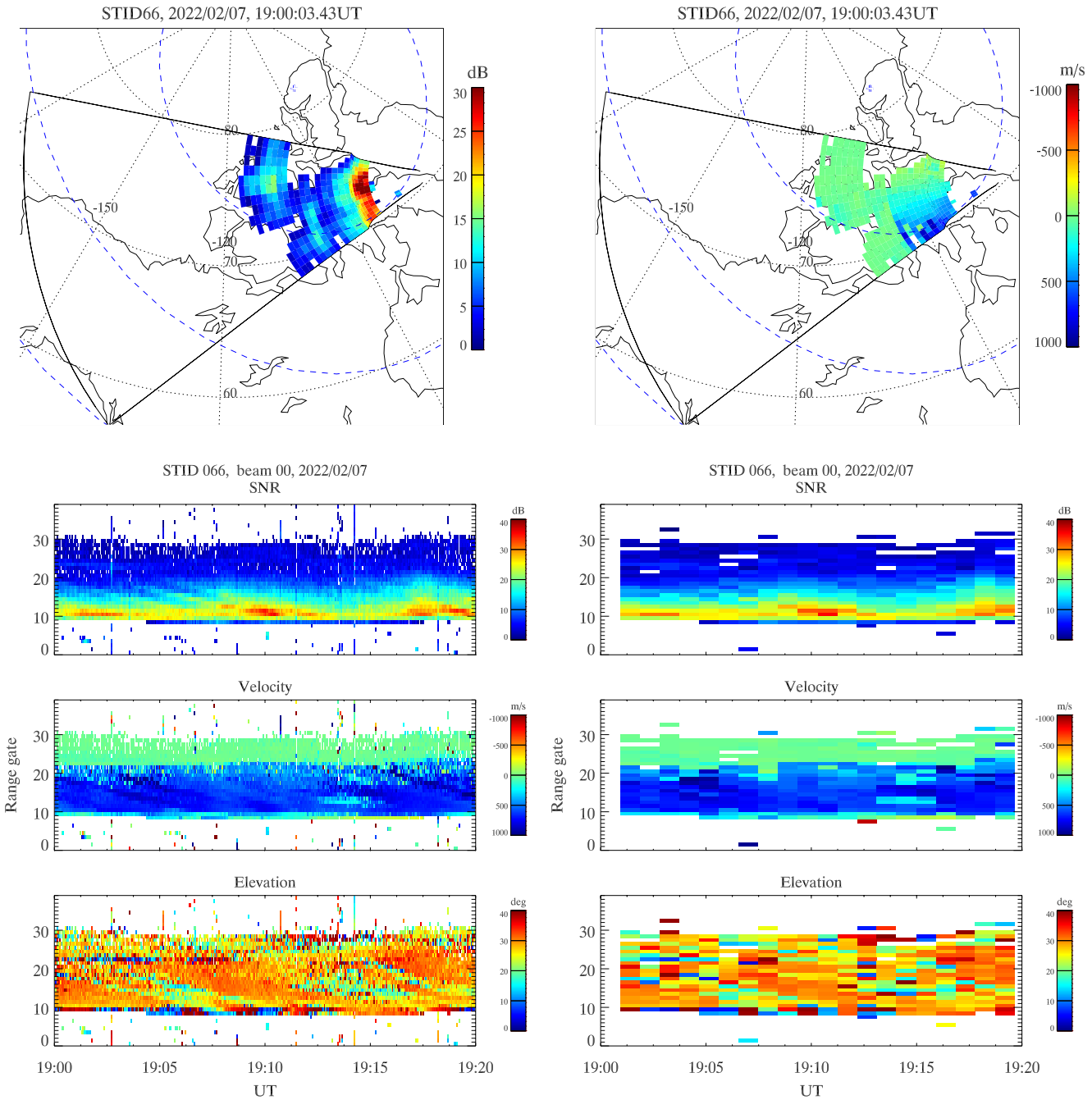

Figure 6. Data from proof-of-concept full field-of-view (FOV) imaging experiment. Fan plots of signal-to-noise ratio (SNR) (top left) and line-of-sight velocity (top right, red—away from the radar, blue—toward the radar) obtained during a wide-beam transmission experiment at CLY on 7 February 2022. Images were obtained every 3.5-s. The bottom three rows are range-time plots of the same data set recorded from 19:00 to 19:20 UT along beam 0, which is the left edge of the FOV. The parameters displayed are SNR (top), line-of-sight velocity (middle), and elevation angle (bottom). The range-time plots on the left contain the imaging data with a 3.5 s sampling rate. The range-time plots on the right contain the same data with the sampling rate reduced to the 1 min resolution of a conventional Super Dual Auroral Radar Network scan.

simultaneously. When these capabilities are realized, it will enhance the measurement quality and resolution. A drawback is that the data storage and processing requirements increase significantly for each additional capability that is implemented. With the rapid advancements in digital storage media and computational processing speeds, we anticipate these factors will become less of a barrier over time and that simultaneous integration of these techniques will be operationalized.

Data Availability Statement

The data used in the study are available at https://doi.org/10.5281/zenodo.7643947.

Acknowledgments
SuperDARN Canada operations are supported by funding from the Canada Foundation for Innovation (CFI), the Canadian Space Agency's (CSA) Geospace Observatory (GO) Canada program, and Innovation Saskatchewan. KM is supported by the NSERC Discovery Grant RGPIN 05472-2017. PP is supported by the CSA Grant 21SUSTMRPI. SuperDARN is a collection of radars funded by national scientific funding agencies of Australia, Canada, China, France, Italy, Japan, Norway, South Africa, United Kingdom and the United States of America. SuperDARN Canada data, including Borealis data, are available from https://superdarn.ca/data-download and are published at the Federated Research Data Repository https://www.frdr-dfdr.ca/repo/collection/superdarn. The authors thank the University of Saskatchewan's Physics Machine shop for custom work. The authors are grateful for radar design discussions with the SuperDARN community, Juha Vierinen, Phil Erickson, Koki Chau, and Brian Bienvenu.

References

Bristow, W. A. (2019). Application of radar imaging analysis to SuperDARN observations. *Radio Science*, *54*(7), 692–703. https://doi.org/10.1029/2019RS006851

Capon, J. (1969). High-resolution frequency-wavenumber spectrum analysis. *Proceedings of the IEEE*, *57*(8), 1408–1418. https://doi.org/10.1109/proc.1969.7278

Chisham, G., Lester, M., Milan, S. E., Freeman, M. P., Bristow, W. A., Grocott, A., et al. (2007). A decade of the Super Dual Auroral Radar Network (SuperDARN): Scientific achievements, new techniques and future directions. *Surveys in Geophysics*, *28*(1), 33–109. https://doi.org/10.1007/s10712-007-9017-8

Cousins, E. D. P., & Shepherd, S. G. (2010). A dynamical model of high-latitude convection derived from superdarn plasma drift measurements. *Journal of Geophysical Research*, *115*(A12), A12329. https://doi.org/10.1029/2010JA016017

Cowley, S. W. H., & Lockwood, M. (1992). Excitation and decay of solar wind-driven flows in the magnetosphere-ionosphere system. *AnGeo*, *10*(1–2), 103–115.

Custovic, E., McDonald, A. J., Whittington, J., Elton, D., Kane, T. A., & Devlin, J. C. (2013). New antenna layout for a SuperDARN HF radar. *Radio Science*, *48*(6), 722–728. https://doi.org/10.1002/2013RS005156

Custovic, E., Nguyen, H. Q., Devlin, J. C., Whittington, J., Elton, D., Console, A., et al. (2011). Evolution of the SuperDARN antenna: Twin terminated folded dipole antenna for HF systems. In *7th International Conference on Broadband Communications and Biomedical Applications* (pp. 24–29). https://doi.org/10.1109/IB2Com.2011.6217936

Fiori, R. A. D., Boteler, D. H., Koustov, A. V., Haines, G. V., & Ruohoniemi, J. M. (2010). Spherical cap harmonic analysis of Super Dual Auroral Radar Network (SuperDARN) observations for generating maps of ionospheric convection. *Journal of Geophysical Research*, *115*(A7), A07307. https://doi.org/10.1029/2009JA015055

Frerking, M. E. (1994). *Digital signal processing in communications systems*. Springer.

Gjerloev, J. W., Waters, C. L., & Barnes, R. J. (2018). Deriving global convection maps from SuperDARN measurements. *Journal of Geophysical Research: Space Physics*, *123*(4), 2902–2915. https://doi.org/10.1002/2017JA024543

Gray, R. W., & Farley, D. T. (1973). Theory of incoherent-scatter measurements using compressed pulses. *Radio Science*, 8(2), 123–131. https://doi.org/10.1029/RS008i002p00123

Greenwald, R. A., Baker, K. B., Dudeney, J. R., Pinnock, M., Jones, T. B., Thomas, E. C., et al. (1995). DARN/SuperDARN: A global view of the dynamics of high-latitude convection. *Space Science Reviews*, *71*(1), 761–796. https://doi.org/10.1007/BF00751350

Greenwald, R. A., Baker, K. B., Hutchins, R. A., & Hanuise, C. (1985). An HF phased-array radar for studying small-scale structure in the high-latitude ionosphere. *Radio Science*, *20*(1), 63–79. https://doi.org/10.1029/rs020i001p00063

Harding, B. J., & Milla, M. (2013). Radar imaging with compressed sensing. *Radio Science*, *48*(5), 582–588. https://doi.org/10.1002/rds.20063

Hysell, D. L. (1996). Radar imaging of equatorial F region irregularities with maximum entropy interferometry. *Radio Science*, *31*(6), 1567–1578. https://doi.org/10.1029/96RS02334

Kelley, M. C. (2009). *The Earth's ionosphere: Plasma physics and electrodynamics*. Academic Press, Inc.

Lehtinen, M. S., Huuskonen, A., & Markkanen, M. (1997). Randomization of alternating codes: Improving incoherent scatter measurements by reducing correlations of gated autocorrelation function estimates. *Radio Science*, *32*(6), 2271–2282. https://doi.org/10.1029/97RS02556

Lester, M. (2014). The Super Dual Auroral Radar Network (SuperDARN): An overview of its development and science. *Advances in Polar Science*, *24*, 1–11. https://doi.org/10.3724/SP.J.1085.2013.00001

Lester, M., Chapman, P. J., Cowley, S. W. H., Crooks, S. J., Davies, J. A., Hamadyk, P., et al. (2004). Stereo cutlass – A new capability for the SuperDARN HF radars. *Annales Geophysicae*, *22*(2), 459–473. https://doi.org/10.5194/angeo-22-459-2004

Nishitani, N., Ruohoniemi, J. M., Lester, M., Baker, J. B. H., Koustov, A. V., Shepherd, S. G., et al. (2019). Review of the accomplishments of mid-latitude Super Dual Auroral Radar Network (SuperDARN) HF radars. *Progress in Earth and Planetary Science*, *6*(1), 1–57. https://doi.org/10.1186/s40645-019-0270-5

NVIDIA. (2016). *Cuda C++ programming guide* (Tech. Rep.). NVIDIA Corporation. Retrieved from https://developer.nvidia.com/cuda-toolkit-archive

Ponomarenko, P. V., & Waters, C. L. (2006). Spectral width of SuperDARN echoes: Measurement, use and physical interpretation. *Annals of Geophysics*, *24*(1), 115–128. https://doi.org/10.5194/24-115-2006

Ponomarenko, P. V., Waters, C. L., & Menk, F. W. (2007). Factors determining spectral width of HF echoes from high latitudes. *Annales Geophysicae*, *25*(3), 675–687. https://doi.org/10.5194/angeo-25-675-2007

Richards, M., Scheer, J., & Holm, W. (2010). *Principles of modern radar: Basic principles*. Scitech Publishing.

Ruohoniemi, J. M., & Greenwald, R. A. (1996). Statistical patterns of high-latitude convection obtained from Goose Bay HF radar observations. *Journal of Geophysical Research*, *101*(A10), 21743–21763. https://doi.org/10.1029/96ja01584

Rytov, S. M., Kravtsov, Y. A., & Tatarskii, V. I. (1988). *Principles of statistical radiophysics* (Vol. 4). Springer-Verlag.

Shepherd, S. G., Sterne, K. T., Thomas, E. G., Ruohoniemi, J. M., Baker, J. B. H., Parris, R. T., et al. (2020). Bistatic observations with SuperDARN HF radars: First results. *Radio Science*, *55*(8), e2020RS007121. https://doi.org/10.1029/2020RS007121

Spaleta, J., Bristow, W. A., & Klein, J. (2015). Temporal and spatial resolved SuperDARN line of sight velocity measurements corrected for plasma index of refraction using Bayesian inference. *Journal of Geophysical Research: Space Physics*, *120*(4), 3207–3225. https://doi.org/10.1002/2014JA020960

Sterne, K. T., Greenwald, R. A., Baker, J. B., & Ruohoniemi, J. M. (2011). Modeling of a twin terminated folded dipole antenna for the Super Dual Auroral Radar Network (SuperDARN). In *2011 IEEE RadarCon (RADAR)* (pp. 934–938). https://doi.org/10.1109/RADAR.2011.5960673

SuperDARN Canada. (2022). *Borealis documentation* (Tech. Rep.). University of Saskatchewan. Retrieved from https://borealis.readthedocs.io/

The HDF Group. (1997–2020). Hierarchical data format, version 5. Retrieved from https://www.hdfgroup.org/solutions/hdf5/

Thomas, E. G., & Shepherd, S. G. (2018). Statistical patterns of ionospheric convection derived from mid-latitude, high-latitude, and polar SuperDARN HF radar observations. *Journal of Geophysical Research: Space Physics*, *123*(4), 3196–3216. https://doi.org/10.1002/2018JA025280

Whittington, J., Devlin, J., & Nguyen, M. (2004). Digital stereo enhancement to the TIGER radar system. In *Proceedings of the Workshop on Applications of Radio Science (WARS'04), Hobart, Tasmania*.

Yan, J., Deng, X., Lan, A., Wu, J., Zhang, J., Wang, W., & Qiu, H. (2021). The digital beam forming technique in AgileDARN high-frequency radar. *Polar Science*, *28*, 100595. https://doi.org/10.1016/j.polar.2020.100595